Trapping light in polymer photodiodes with soft embossed gratings

Roman, L.S.; Inganäs, O; Granlund, T.; Nyberg, T.; Svensson, M.; Andersson, M.R.; Hummelen, J.C.; Inganas, O

Published in:
Advanced materials

DOI:
10.1002/(SICI)1521-4095(200002)12:3<189::AID-ADMA189>3.0.CO;2-2

Publication date:
2000

ADVANCED MATERIALS

Similar networking structures were also obtained with gold particles where multiple copies of dithiols were exchanged into the protecting monolayers prior to LB compression, as well as with other metal particles such as alkanethiolate-protected palladium particles.[29] By using the air/water interface as the substrate, networking structures of metal as well as semiconductor nanoparticles can, in principle, be constructed by the above approach with appropriate bifunctional linkers. With monodisperse particles, it is likely that a macroscopic superlattice network can be fabricated, where the particle distribution can be manipulated by, for instance, the linker chain length. The resulting assemblies can then easily be deposited onto solid substrate surfaces and serve as the structural basis for the construction of more complicated nanocomposite structures, on which further investigations can be carried out, for instance, anisotropic electron-transfer (hopping) kinetics, optoelectronic properties, and nanoparticle-based lithography.[30]

To conclude, 2D crosslinked nanoparticle networks were fabricated by the Langmuir–Blodgett technique where the bridging of neighboring particles was effected by rigid dithiol linkers, resulting in macroscopic patches of particles visible on the air/water interface even at low surface pressure. TEM measurements revealed close-packed particle assemblies, consistent with the red-shift observed in the optical spectroscopy measurements.

Experimental

1-Hexanethiolate-protected gold (C6Au) nanoparticles were synthesized in a biphasic system, as reported previously [12,13]. The particles were then partially fractionated using a mixture of toluene and ethanol [31], with the final gold cores consisting of roughly 145 gold atoms (average core diameter 1.6 nm) [13]. 4,4′-Thiobisbenzenethiol (from Aldrich) and all solvents were used as received. LB studies were conducted at room temperature on a Nima 611D Langmuir–Blodgett trough with a Welhelmy plate as the surface-pressure sensor and nanopure water (supplied by a Barnstead Nanopure water system, 18.3 MΩ) as the subphase. A solution (0.08 mM) of the fractionated particles was prepared in hexane while TBBT was dissolved in chloroform to make a concentration of ca. 2.4 mM. The calculated amount of the solutions was cast dropwise onto the water surface using a Hamilton microliter syringe. At least 20 min was allowed for evaporation prior to isotherm measurement and between compressions. Two particle layers were deposited onto both sides of a cleaned glass slide at a surface pressure $\pi = 13$ mN/m. Optical measurements were carried out with a Unicam ATI UV-4 spectrometer with a resolution of 2 nm. The surface-plasmon band positions were determined by the second-order derivatives of the spectra. The TEM study was carried out with a Hitachi H7100 microscope (75 keV). Typically phase-contrast micro-images were captured at 300 K to 400 K magnification.

Received: July 20, 1999
Final version: September 8, 1999

[1] M. Burghard, G. Philipp, S. Roth, K. von Klitzing, R. Pugin, G. Schmid, *Adv. Mater.* **1998**, *10*, 842.
[2] S.-R. Yeh, M. Seul, B. I. Shraiman, *Nature* **1997**, *386*, 57.
[3] M. Trau, D. A. Saville, I. A. Aksay, *Science* **1996**, *272*, 706.
[4] C. P. Collier, R. J. Saykally, J. J. Shiang, S. E. Henrichs, J. R. Heath, *Science* **1997**, *277*, 1978.
[5] W.-Y. Lee, M. J. Hostetler, R. W. Murray, M. Majda, *Isr. J. Chem.* **1997**, *37*, 213.
[6] K. C. Yi, Z. Hórvölgyi, J. H. Fendler, *J. Phys. Chem.* **1994**, *98*, 3872.
[7] M. Giersig, P. Mulvaney, *Langmuir* **1993**, *9*, 3408.
[8] Z. L. Wang, *Adv. Mater.* **1998**, *10*, 13.
[9] G. Schmid, *Clusters and Colloids: From Theory to Applications*, VCH, Weinheim, Germany **1994**.
[10] H. Haberland, *Clusters of Atoms and Molecules*, Springer, New York **1994**.
[11] M. A. Hayat, *Colloidal Gold: Principles, Methods and Applications*, Academic Press, New York **1989**, Vol. 1.
[12] M. Brust, M. Walker, D. Bethell, D. J. Schiffrin, R. Kiely, *J. Chem. Soc., Chem. Commun.* **1994**, 801.
[13] M. J. Hostetler, J. E. Wingate, C.-H. Zhong, J. E. Harris, R. W. Vachet, M. R. Clark, J. D. Londono, S. J. Green, J. J. Stokes, G. D. Wignall, G. L. Glish, M. D. Porter, N. D. Evans, R. W. Murray, *Langmuir* **1998**, *14*, 17.
[14] S. Chen, R. S. Ingram, M. J. Hostetler, J. J. Pietron, R. W. Murray, T. G. Schaaff, J. T. Khoury, M. M. Alvarez, R. L. Whetten, *Science* **1998**, *280*, 2098.
[15] R. S. Ingram, M. J. Hostetler, R. W. Murray, T. P. Bigioni, D. K. Guthrie, P. N. First, *J. Am. Chem. Soc.* **1997**, *119*, 9279.
[16] S. Chen, R. W. Murray, S. W. Feldberg, *J. Phys. Chem. B* **1998**, *102*, 9898.
[17] S. Chen, R. W. Murray, *J. Phys. Chem. B* **1999**, *103*, 9996.
[18] M. Gao, B. Richter, S. Kristein, *Adv. Mater.* **1997**, *9*, 802.
[19] C. B. Murray, C. R. Kagan, M. G. Bawendi, *Science* **1995**, *270*, 1335.
[20] T. Torimoto, N. Tsumura, M. Miyake, M. Nishizawa, T. Sakata, H. Mori, H. Yoneyama, *Langmuir* **1999**, *15*, 1853.
[21] M. Brust, D. Bethell, D. J. Schiffrin, C. J. Kiely, *Adv. Mater.* **1995**, *7*, 795.
[22] M. J. Hostetler, A. C. Templeton, R. W. Murray, *Langmuir* **1999**, *15*, 3782.
[23] M. Kerker, *The Scattering of Light and Other Electromagnetic Radiation*, Academic Press, New York **1969**.
[24] C. F. Bohren, D. R. Huffmann, *Absorption and Scattering of Light by Small Particles*, Wiley, New York **1983**, Ch. 12.
[25] S. Underwood, P. Mulvaney, *Langmuir* **1994**, *10*, 3427.
[26] The appearance of a second absorption peak (at ca. 516 nm, Fig. 2) in the optical measurement was caused by data smoothing with Peakfit.
[27] M. P. Pileni, *New J. Chem.* **1998**, 693.
[28] C. A. Mirkin, R. L. Letsinger, R. C. Mucic, J. J. Storhoff, *Nature* **1996**, *382*, 607.
[29] S. Chen, K. Huang, J. A. Stearns, *Chem. Mater.*, in press.
[30] C. P. Collier, T. Vossmeyer, J. R. Heath, *Annu. Rev. Phys. Chem.* **1998**, *49*, 371.
[31] T. G. Schaaff, M. N. Shafigullin, J. T. Khoury, I. Vezmar, R. L. Whetten, W. G. Cullen, P. N. First, C. Gutiérrez-Wing, J. Ascensio, M. J. Jose-Yacamán, *J. Phys. Chem. B* **1997**, *101*, 7885.

Trapping Light in Polymer Photodiodes with Soft Embossed Gratings**

By *Lucimara Stolz Roman*,* *Olle Inganäs*,* *Thomas Granlund*, *Tobias Nyberg*, *Mattias Svensson*, *Mats R. Andersson*, and *Jan C. Hummelen*

Conjugated polymers are an attractive choice for use in electronic devices. Polymeric transistors,[1] light-emitting

[*] L. S. Roman, Dr. O. Inganäs, T. Granlund, T. Nyberg
Laboratory of Applied Physics, Department of Physics (IFM)
Linköping University
SE-581 83 Linköping (Sweden)
M. Svensson, Dr. M. R. Andersson
Department of Polymer Technology
Chalmers University of Technology
SE-41296, Göteborg (Sweden)
Dr. J. C. Hummelen
Stratingh Institute & MSC, University of Groningen
Nijenborgh 4, NL-9747 AG Groningen (The Netherlands)

[**] The authors acknowledge the financial support of the Göran Gustafsson foundation Sweden and thank L. A. A. Pettersson for valuable discussions.

  0935-9648/00/0302-0189 $ 17.50+.50/0

diodes (LEDs),[2,3] diodes,[4] photodiodes,[5,6] and solar cells[7] with promising performance indicators have been developed. Further work to optimize these materials for electronic applications is in progress. To obtain functional microelectronic devices it is necessary to pattern the active semiconductor layers and the electrodes. In conventional silicon technology this is done using standard photolithography processing. These patterning methods are not suitable for polymers because the surface could be exposed to solvents or UV light, which might cause material degradation. The need to develop special patterning techniques for polymers is important, and here soft lithography offers alternatives. Soft lithography is a set of gentle processes that can be used for patterning in polymeric devices: micro-contact printing,[8] replica molding,[9] self-assembled monolayers,[10] and put-down and lift-up techniques.[11] Printing of electrodes with elastomer stamps has been used to produce arrays of LEDs.[11] These structures were well beyond 1 μm in dimensions. Here we demonstrate another soft lithography technique, soft embossing, for patterning submicrometer topographical features on large areas of an active polymer layer. This grating is used to enhance the performance of polymer photodiodes by trapping light into the polymer film.

In the creation of conjugated polymer photovoltaic devices, a limiting aspect of the device physics is the short diffusion length of excited states in conjugated polymers, typically in the range 5–10 nm.[12] The optical absorption of conjugated polymers is strong, but even at the maximum absorption, the penetration depth of light into these materials is in the range 10–100 nm. We therefore have to combine the generation of excited states over 10–100 nm depth and harvesting, which occurs over a much shorter distance. The dissociation of excited states, necessary for creating charge carriers, occurs at interfaces, impurities, or in strong electric fields. Efficient charge generation can occur if all excited states can find a dissociating site close enough; this is done in the distributed donor–acceptor networks[13,14] based on combination of conjugated polymers and efficient acceptors such as C_{60}. The use of asymmetric contacts of different work function gives a built-in electric field to separate the charge carriers and extract a photocurrent. By making thicker polymer layers, to collect more of the light by absorption, we also decrease the field and reduce the collection efficiency, forcing us to compromise the photocurrent.[15] It is therefore desirable to make very thin devices, but to find ways of enhancing the absorption in these polymer layers.

One way of reconciling these different requirements is to trap light into the polymer layers by diffraction into guided modes in the thin polymer films. This approach has been used to enhance light trapping and absorption in silicon solar cells,[16] particularly in the energy range where optical absorption in silicon is low, thus increasing the conversion efficiency.[17] Theoretical results show that a 5 μm Si cell with a staircase grating has about the same absorption as a 20-times thicker cell with a planar reflector.[18] While optical absorption in the conjugated polymers is high, we attempt to use a similar approach in order to trap light into the thinner polymer films.

We have used an elastomeric mold to transfer a submicrometer grating pattern from a commercially available grating template to the active polymer layer in a photovoltaic device. The topography of the polymer layer is now a grating, with a period defined by the template and a grating depth defined by processing conditions. An evaporated metal is used as the electrode and follows the topography of the polymer surface. We were able to find proper coupling conditions for the grating device, thus enhancing the absorption in the active layer and bringing up its efficiency. To analyze the effects of the grating pattern, we studied the spectral response using incident light with two states of polarization, as well as the dependence of the photocurrent on the angle of incident light.

The fabrication of elastomeric molds with a patterned submicrometer grating is presented schematically in the upper part of Figure 1. The polysiloxane pre-polymer (Sylgard 184, Dow Corning Corporation) was poured onto a commercial metallic grating template and then cured at 60 °C for 24 h. The rubber was easily peeled off the grating after curing. The rubber was then taken to the scanning force microscope (SFM, Nanoscope III, Digital Instruments) where the pattern could be seen clearly, as shown in image to the right. The grating template reproduced was sinusoidal with 3600 lines per millimeter. The photovoltaic devices were fabricated in a sandwich structure with a transparent layer of PEDOT(PSS) (poly(3,4-ethylenedioxythiophene), Baytron, Bayer AG, doped with polystyrene sulfonate), as the hole collector electrode using an indium-tin-oxide (ITO) (120 nm) or gold (6 nm) under-layer in order to decrease the series resistance in the device. Aluminum was used as the electron collector electrode. Two active polymer layers were used, one was the semiconducting polymer PTOPT (poly(3,4-octylphenyl)2,2-bithiophene),[19] deposited by spin coating onto ITO/PEDOT(PSS) electrode, from a chloroform solution, with a thickness of 60 nm. The second was a blend of PTOPT with a substituted fullerene [6,6] PCBM ([6,6] phenyl-C_{61}-butyric acid methyl ester)[20] in the ratio 1:2, it was deposited by spin coating onto the Au/PEDOT(PSS) electrode from a toluene solution; the thickness was 90 nm.

To pattern the polymer, the patterned elastomer replica was put in conformal contact with half of the active polymeric film area, as shown in the sequence at the bottom of Figure 1, and the assembly was brought to the polymer softness transition temperature, 80 °C. After cooling, the stamp was removed, and left the grating pattern on the polymer surface. We noted that if patterning is done at higher temperatures (beyond 120 °C), the polymer film will adhere to the elastomer and become difficult to remove. The second electrode Al was vacuum evaporated through a shadow mask defining the active area for two electrodes,

  0935-9648/00/0302-0190 $ 17.50+.50/0

ADVANCED MATERIALS

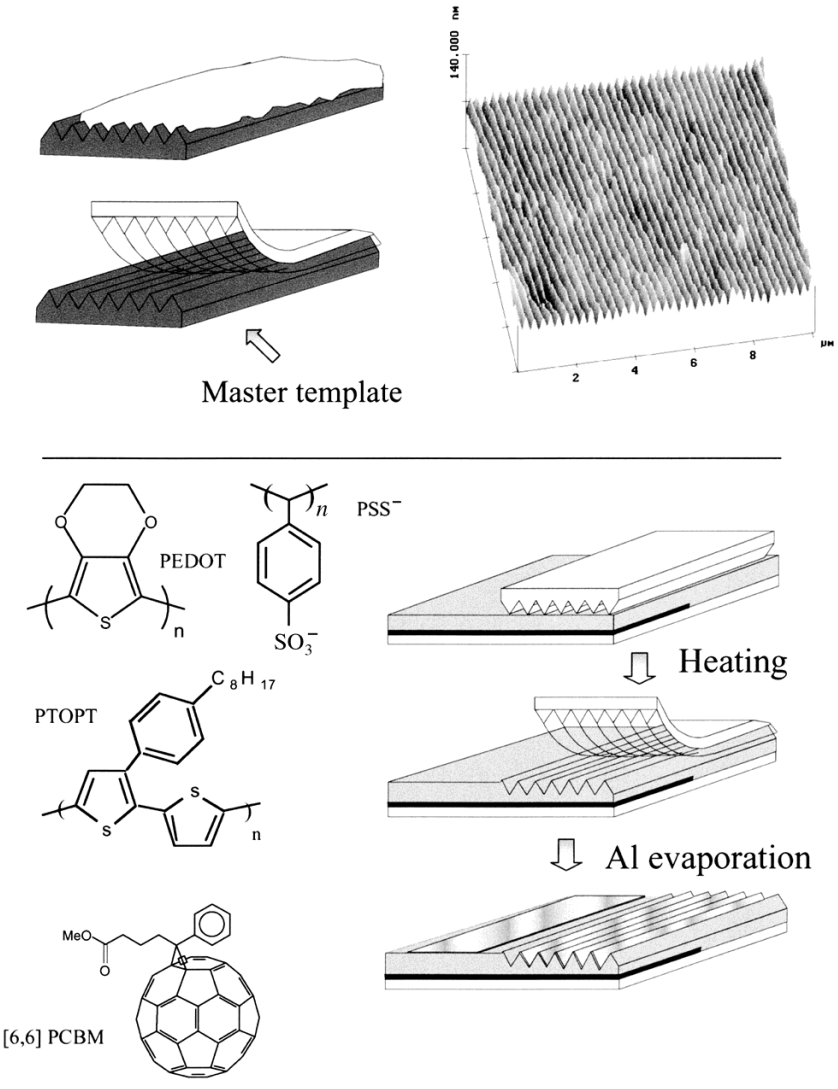

Fig. 1. Fabrication of elastomeric molds with patterned submicrometer grating. The liquid pre-polymer polysiloxane is poured onto a commercial grating and after curing it is peeled off. The SFM image shows the resulting pattern in the rubber. The grating pattern is transferred to the surface of an active polymer layer by soft embossing. The rubber stamp is left in conformal contact with the polymer layer in the softness transition. After cooling, the stamp is peeled off leaving the pattern on the polymer surface. Only half of the polymer area is patterned for reference measurements. The conducting polymer PEDOT(PSS) is used as the anode, the active layers were formed by the semiconducting polymer PTOPT alone or in a blend with [6,6] PCBM.

one onto the grating and the other just onto the flat polymer surface, in order to have a reference measurement for the photoelectric behavior. We call these the grating and the reference photodiode, respectively. The action spectra were taken by measuring the short circuit current using a Keithley 485 picoammeter under monochromatic illumination from an Oriel 257 monochromator with a tungsten halogen lamp.

We investigated both the neat polymer and a distributed donor–acceptor polymer/fullerene material in these grating structures. In the simplest system, the single PTOPT layer device, the photon-to-current efficiency was low, but was improved by the patterned electrode. Likewise we observed an enhancement of photocurrent in the patterned structures incorporating the PTOPT/PCBM blend, where we started from much higher photocurrents due to the highly efficient photoinduced charge transfer between polymer and acceptor.

The action spectra of the photodiodes, the ratio between photocurrent density and photon flow per area (external quantum efficiency, EQE), of the PTOPT single layer device with and without the grating, under normal light incidence is shown in Figure 2. The efficiency at the maximum peak position of the PTOPT absorption spectrum for the grating diode is 30 % higher than the reference. The efficiency enhancement in the grating device can be observed all over the wavelength range with a specific resonance, a shoulder at 420 nm. In the second device, now with a different grating and the PTOPT/PCBM blend, a thin transparent gold layer rather than ITO and a thicker polymer blend film was used. The efficiency increased drastically with the introduction of fullerenes into PTOPT, making the measurements easier. In the spectral response of the grating and reference diodes under normal incidence (Fig. 3) we notice the enhancement in efficiency all over the spectrum with the grating photodiode. At maximum peak position the enhancement of EQE was around 26 %. In this system no resonant peak was found for the wavelength range investigated.

The amount of enhancement in photocurrent and the resonance peak position are qualities of the grating defined by the geometrical properties of the grating and device geometry. Among the parameters involved is the index of refraction, the thickness of the different layers, the absorption coefficient of every layer in the device, the grating shape, period, and depth. As the optical constants of the different layers show dispersion, and in the case of polymers also anisotropy,[21] the modeling is a subtle exercise. For one thing, we do not expect to be able to observe the sharp resonance found in the first order modeling: dispersion in the optical constants and irregularities in the grating will certainly forbid this. This will assist us in our goal—to make a broadband collection of photons in order to increase the photocurrent.

In the neat polymer device, the grating profile on the PTOPT surface was imaged with SFM (Fig. 2). The sinusoidal shape and the period of 277 nm (see cross-section) is given by the master template used (Fig. 1) and the depth

  0935-9648/00/0302-0191 $ 17.50+.50/0

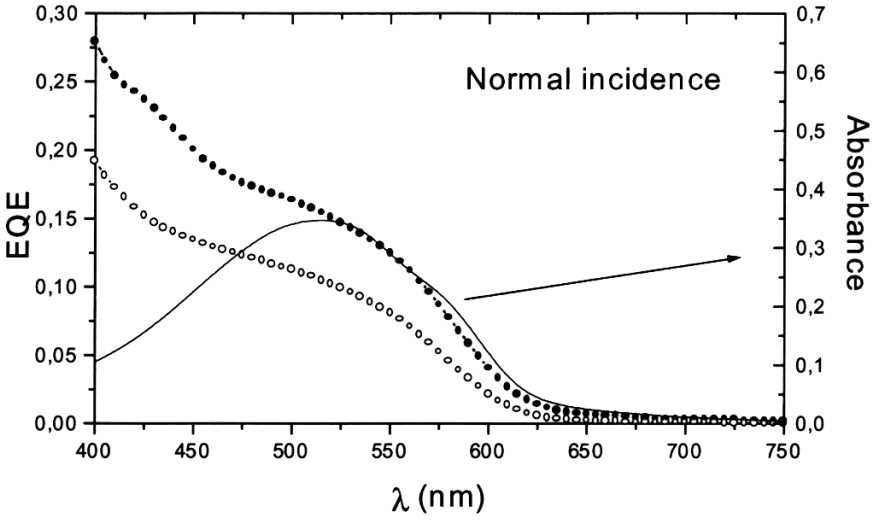

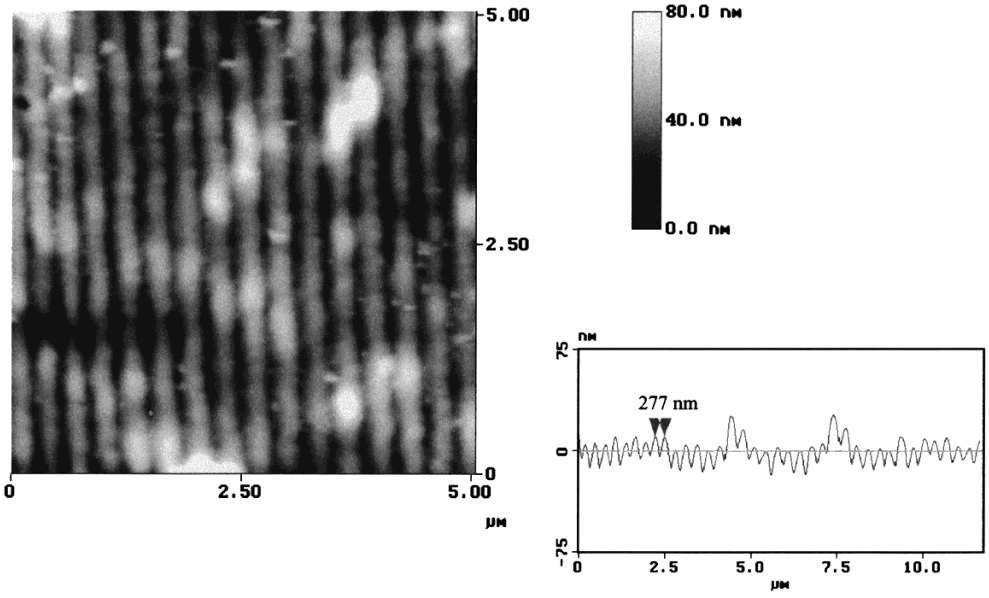

Fig. 2. Action spectra of ITO/PEDOT(PSS)/PTOPT/Al device with (●) and without (○) grating. The absorption spectrum of PTOPT polymer is plotted as a solid line. The measurements are performed on the same sample, using different Al contacts onto flat and patterned polymer surface. The efficiency of the patterned diode is greater than that of the planar one. The grating couples to the device, improving the absorption, creating a shoulder with the maximum in the wavelength of 420 nm. The SFM image shows the patterned PTOPT polymer layer. The grating period, 277 nm, is shown in the cross-section.

(here around 17 nm) is dependent on the pressure applied during the embossing. The index of refraction and the absorption coefficient were measured by spectroscopic ellipsometry, and the layer thickness with a Sloan Dektak 3030 profilometer. In preliminary optical modeling we found that in this device the ITO layer is coupled with the grating because of the high value for the index of refraction in ITO. Although the main light confinement was into the ITO layer, the collateral effect was an enhancement of absorption in the PTOPT layer. The photoresponse behavior is quite sensitive to variations in grating and device geometry. When changing from neat polymer to the blend for the active layer, the thickness and index of refraction value of the active layer caused a different grating–device coupling, thus diminishing the photocurrent value of the grating diode compared to the reference. We therefore chose to use an Au/PEDOT(PSS) electrode in the PTOPT/PCBM device. Even though the gold electrode presents high losses due to reflections at the glass–gold interface, the light trapping in the active layer was improved. The pattern on the blend was a triangular shaped grating with 2400 lines per millimeter, giving a period of 416 nm. The grating profile on the polymer surface imaged by SFM (the bottom part of Fig. 3) confirms the shape and period of the

  0935-9648/00/0302-0192 $ 17.50+.50/0

ADVANCED MATERIALS

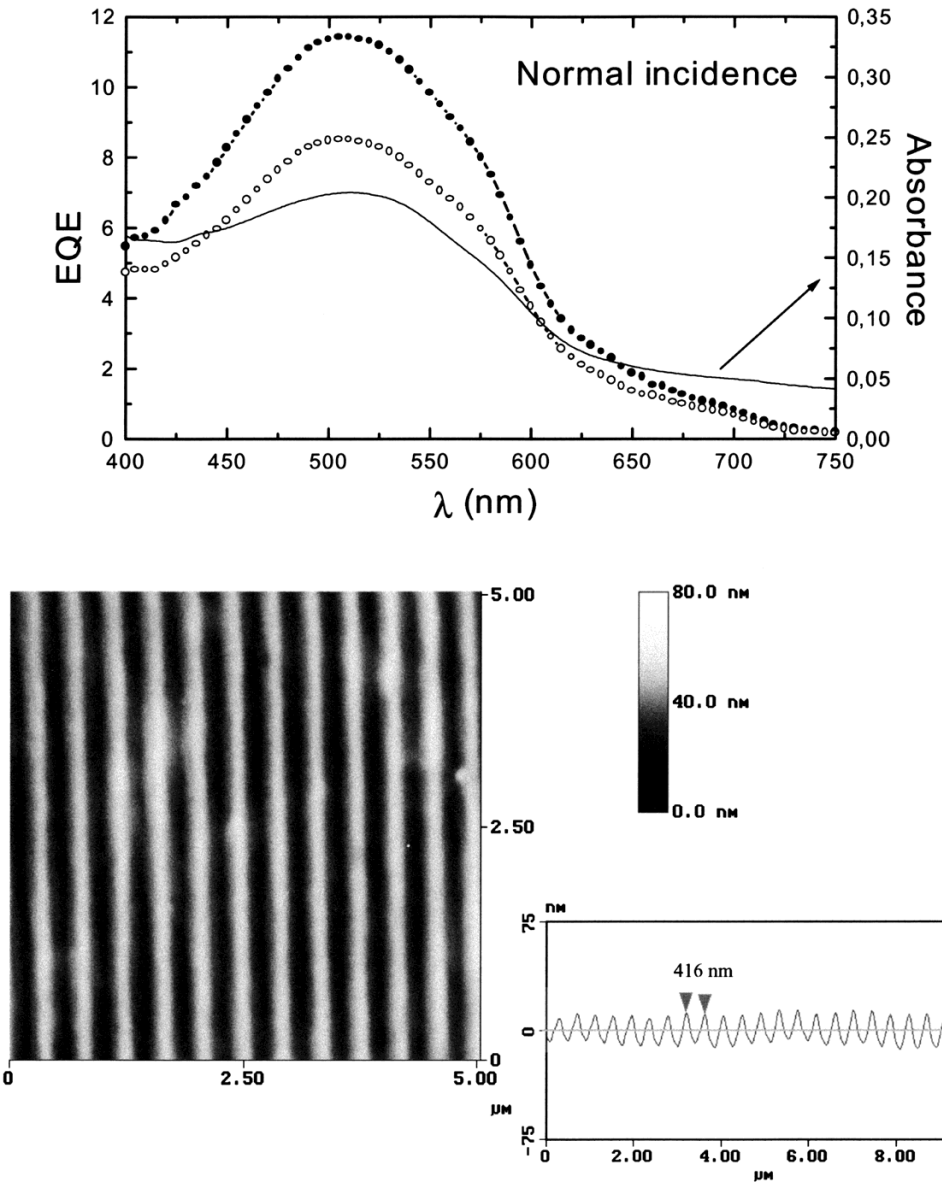

Fig. 3. Action spectra of Au/PEDOT(PSS)/PTOPT:[6,6] PCBM (1:2)/Al device with (●) and without (○) grating. The absorption spectrum of the PTOPT:PCBM 1:2 blend is plotted as a solid line. The measurements are performed on the same sample, using different Al contacts onto flat and patterned polymer surface. The efficiency of the patterned diode is higher than that of the flat one. The SFM image is taken from the patterned blend polymeric layer. The grating period, 416 nm, is shown in the cross-section.

master; the depth of the embossed grating was 15 nm (cross-section).

Having observed the desired enhancement of efficiency in the grating diodes, we wish to verify whether this is due to the presence of the grating or not. By using polarized light, we were able to align the grating direction parallel or transverse to the state of polarization, and thus make the grating decisive or unimportant with respect to the propagation of light in the layers. By varying the angle of incident light, we could also vary the coupling efficiency of the grating.

The grating influence was investigated in experiments using incident polarized light in two orthogonal states of polarization, transverse and parallel, with respect to the grating lines. In Figures 4a,b are presented the action spectra of the grating and reference diodes under normal light incidence in transverse and parallel light polarization, for polymer and polymer blend devices, respectively. Both devices have sublinear dependence of photocurrent on light intensity, which resulted in higher photoconversion efficiency under lower light intensity, as the polarized light has half of the ordinary light intensity from the monochromator. The parallel mode excites the grating coupling, thereby trapping light and improving photoconversion. In transverse mode we observe no strong influence of the grating, but we observe that the grating diode still exhibits higher

  0935-9648/00/0302-0193 $ 17.50+.50/0

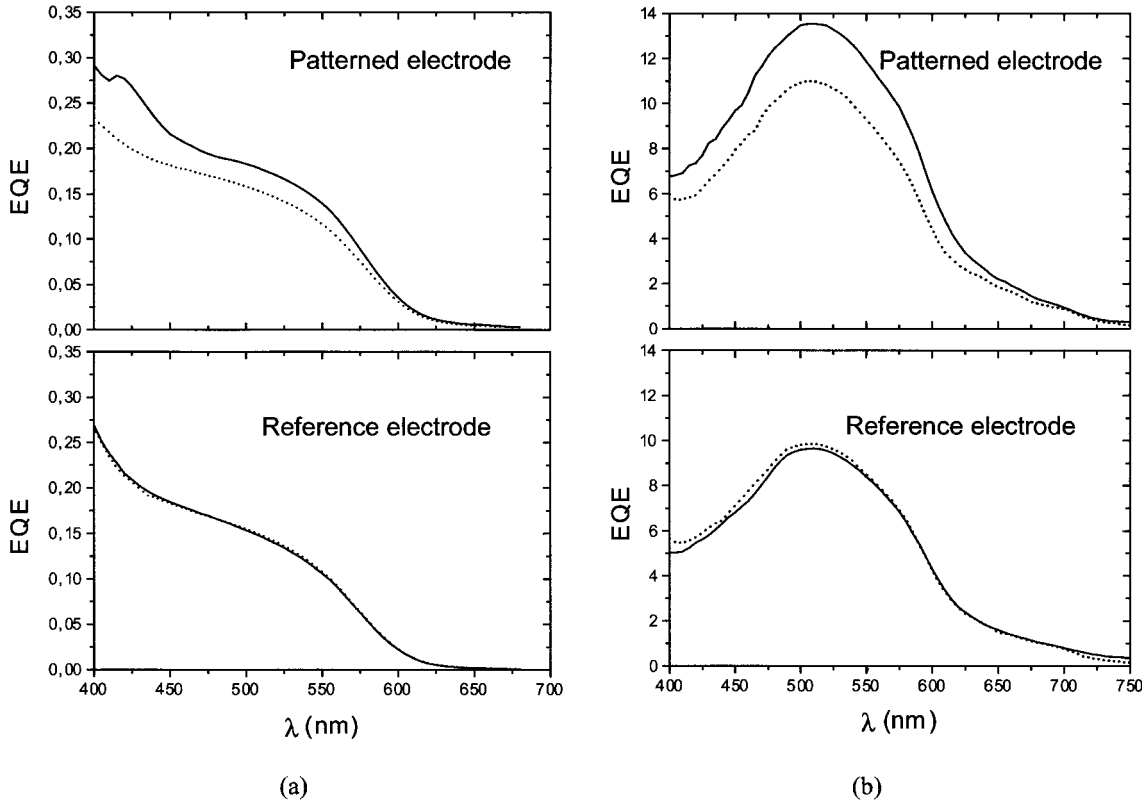

Fig. 4. Measurements of action spectra of: a) ITO/PEDOT(PSS)/PTOPT/Al and b) Au/PEDOT(PSS)/PTOPT:[6,6]PCBM (1:2)/Al devices in the patterned (top) and flat (bottom) electrodes under two orthogonal states of light polarization parallel (solid line) and transverse (dashed line) under normal light incidence.

photocurrent (mainly above 450 nm), probably because of the decrease in the polymer thickness at the valleys of the grating pattern, thus increasing the field and the charge collection. This is more visible in the case of a blended material (Fig. 4b) where the exciton dissociation and charge collection are more effective. The increase of the area of the polymer–metal interface due to the grating is less than 1 % compared to the ordinary area. The reference diodes in both devices presented equal action spectra under both states of polarization. In the case of a single layer device (Fig. 4a) the peak at 420 nm is again present for the parallel light polarization, but disappears for transverse polarization. For the polymer blend device, we do not observe a resonant peak. Preliminary predictions from optical modeling suggest that resonance would appear beyond 700 nm. In this range there is little absorption in the polymer, but appreciable absorption in the gold; therefore we cannot observe a resonant contribution to the photocurrent.

When varying both angle of incident light as well as using transverse and parallel polarization states, in the neat polymer device we note the resonant peak moving with the angle of light incidence. Under parallel polarization and 70° incidence the efficiency was more than four times higher for almost all the wavelength range. Beyond 70° incidence, the reference diode presented a very small photocurrent while the grating diode was still able to absorb light delivering an appreciable photocurrent. Similar behavior was found for the blend device in experiments of spectral response dependence on angle of incidence. We obtained higher improvement in the efficiency ratio (pattern/reference) for higher angles of incidence, under parallel light polarization mode.

In conclusion, these results give strong and direct evidence that the grating function improves the optoelectric properties of photodiodes. The detailed modeling of such grating diodes can be used to optimize performance, something we have not yet attempted; it will require a simultaneous optimization of materials, layer thickness, and grating geometry, under full consideration of the dispersion of optical constants and the possible optical anisotropy of the polymer films. We have demonstrated the possibility of using submicrometer patterning using soft lithography, to implant structure in polymer photodiodes over large areas in order to produce gratings to improve light trapping on thin active layers of polymeric photovoltaic devices. As this simple patterning technique is cheap and suitable for reel-to-reel production over large areas, it may contribute to the goal of efficient photoelectrical energy conversion using organic polymers and molecules.

Received: August 18, 1999
Final version: November 3, 1999

  0935-9648/00/0302-0194 $ 17.50+.50/0

ADVANCED MATERIALS

[1] H. Sirringhaus, N. Tessler, R. H. Friend, *Science* **1998**, *280*, 1741.
[2] N. Tessler, N. T. Harrison, R. H. Friend, *Adv. Mater.* **1998**, *10*, 64.
[3] I. D. Parker, Y. Cao, C. Y. Yang, *J. Appl. Phys.* **1999**, *85*, 2441.
[4] L. S. Roman, M. Berggren, O. Inganäs, *Appl. Phys. Lett.* **1999**, *75*, 3557.
[5] Y. Gang, W. Jian, J. McElvian, A. J. Heeger, *Adv. Mater.* **1998**, *10*, 1431.
[6] L. S. Roman, W. Mammo, L. A. A. Pettersson, M. Andersson, O. Inganäs, *Adv. Mater.* **1998**, *10*, 774.
[7] M. Granström, K. Petrisch, A. C. Arias, A. Lux, M. R. Andersson, R. H. Friend, *Nature* **1998**, *395*, 257.
[8] A. Kumar, G. M. Whitesides, *Appl. Phys. Lett.* **1993**, *63*, 2002.
[9] Y. Xia, E. Kim, X. M. Zhao, J. A. Rogers, M. Prentiss, G. M. Whitesides, *Science* **1996**, *273*, 347.
[10] C. D. Bain, G. M. Whitesides, *Angew. Chem.* **1989**, *101*, 522; *Angew. Chem. Int. Ed. Engl.* **1989**, *28*, 506; *Adv. Mater.* **1989**, *1*, 110.
[11] T. Granlund, T. Nyberg, L. S. Roman, M. Svensson, O. Inganäs, *Adv. Mater* **2000**, in press.
[12] A. Kölher, D. A. dos Santos, D. Beljone, Z. Shuai, J. L. Brédas, A. B. Holmes, A. Kraus, K. Müllen, R. Friend, *Nature* **1998**, *392*, 903.
[13] G. Yu, J. Gao, J. C. Hummelen, F. Wudl, A. J. Heeger, *Science* **1995**, *270*, 1789.
[14] J. J. Halls, C. A. Walsh, N. C. Greenham, E. A. Marseglia, R. H. Friend, S. C. Moratti, A. B. Holmes, *Nature* **1995**, *376*, 498.
[15] L. A. A. Pettersson, L. S. Roman, O. Inganäs, *J. Appl. Phys.* **1999**, *86*, 487.
[16] R. H. Morf, H. Kiess, in *9th E.C. Photovoltaic Solar Energy Conference*, Kluwer, Dordrecht, The Netherlands **1989**.
[17] B. Delley, H. Kiess, *Sol. Energy Mater. Sol. Cells* **1994**, *33*, 1.
[18] R. H. Morf, J. Gobrecht, in *10th Workshop on Quantum Solar Energy Conversion, QUANTSOL'98* (Eds: J. G. W. Kautek, H. Kisch, S. Sariciftci, C. Königstein), European Society for Quantum Solar Energy Conversion, Bad Hofgastein, Austria **1998**.
[19] M. R. Andersson, M. Berggren, O. Inganäs, G. Gustafsson, J. C. Gustafsson-Carlberg, D. Selse, T. Hjertberg O. Wennerström, *Macromolecules* **1995**, *28*, 7525.
[20] J. C. Hummelen, B. W. Knight, F. LePeq, F. Wuld, J. Yao, C. L. Wilkins, *J. Org. Chem.* **1995**, *60*, 532.
[21] L. A. A. Pettersson, S. Ghosh, O. Inganäs, unpublished.

Synthesis of a High-Permeance NaA Zeolite Membrane by Microwave Heating**

By *Xiaochun Xu*, *Weishen Yang*,* *Jie Liu*, and *Liwu Lin*

In the past ten years, many attempts have been made to develop zeolite membranes for separation and catalysis applications.[1–3] Several preparation methods have been developed, such as in-situ hydrothermal synthesis,[4–7] vapor phase transport,[8,9] or embedding microcrystals of the zeolite into a matrix.[10,11] Zeolite membranes prepared by these methods usually have a very good separation factor, but the permeance is too low for practical applications.[12–18] Thus the most challenging work in the field of zeolite membranes is to prepare membranes with high permeance, while keeping the separation factor high.

Recently, a new synthesis method that combines hydrothermal crystallization with the microwave heating technique has been developed.[19–25] Compared with conventional hydrothermal synthesis, microwave synthesis of zeolites has the advantages of very short time, broad composition, small zeolite particle size, narrow zeolite particle size distribution, and high purity. Jansen et al. suggested that these advantages could be attributed to fast homogeneous nucleation and the easy dissolution of the gel.[19]

The formation of a zeolite membrane on a porous support is a heterogeneous nucleation process. First, a gel layer is formed on the porous support surface, followed by nucleation and crystal growth to form a membrane.[26,27] We considered using microwave heating (MH) and conventional heating (CH), which are compared in Figure 1. In the microwave environment, because of the fast, homogeneous

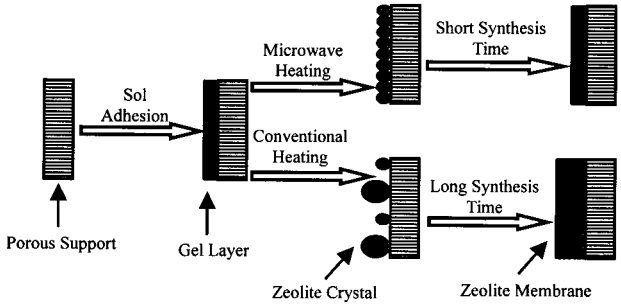

Fig. 1. Comparative synthesis model of zeolite membrane by MH and CH.

heating and the formation of active water molecules,[19] the gel layer at the support–solution interface dissolves quickly, which results in a rapid and more simultaneous nucleation of zeolites on the support surface than if heating conventionally. Moreover, because of the simultaneous nucleation and homogeneous heating, uniformly small zeolite crystals can be synthesized. As a result, thin zeolite membranes can be formed quickly. In the case of CH, the nuclei are not formed on the support surface simultaneously because of the low dissolution rate of the gel and the low heating rate. Thus the zeolite crystals formed are also not uniform in size. In order to form a dense membrane, a long synthesis time will be needed and the membrane will be thick. Therefore, a zeolite membrane synthesized by MH will be thinner and have a higher permeance than one synthesized by CH. Up to now, there have been few reports on the preparation of zeolite membranes by MH,[28–31] and no gas permeation data have been reported. In this communication, the synthesis of a NaA zeolite membrane by MH and its gas permeation properties are presented.

A comparative study on the formation of NaA zeolite membranes by CH and MH was performed. Figure 2A shows the X-ray diffraction patterns of the membrane synthesized by MH for 15 min. The diffraction patterns for the resulting membrane were represented by the sum of the peaks of the α-Al_2O_3 support and the NaA zeolite. It implied that the membrane formed on the α-Al_2O_3 support was the NaA zeolite membrane. Figures 2B–D show the X-ray diffraction patterns of the membranes synthesized by CH for 2, 3, and 4 h respectively. Only the diffraction patterns of NaA zeolite and α-Al_2O_3 support appear in

[*] Prof. W. Yang, Dr. X. Xu, Dr. J. Liu, Prof. L. Lin
State Key Laboratory of Catalysis
Dalian Institute of Chemical Physics
Chinese Academy of Sciences
Dalian 116023 (China)

[**] This work was supported by the National Advanced Materials Committee of China (715-006-0122) and the NSFC (59789201).

  0935-9648/00/0302-0195 $ 17.50+.50/0